

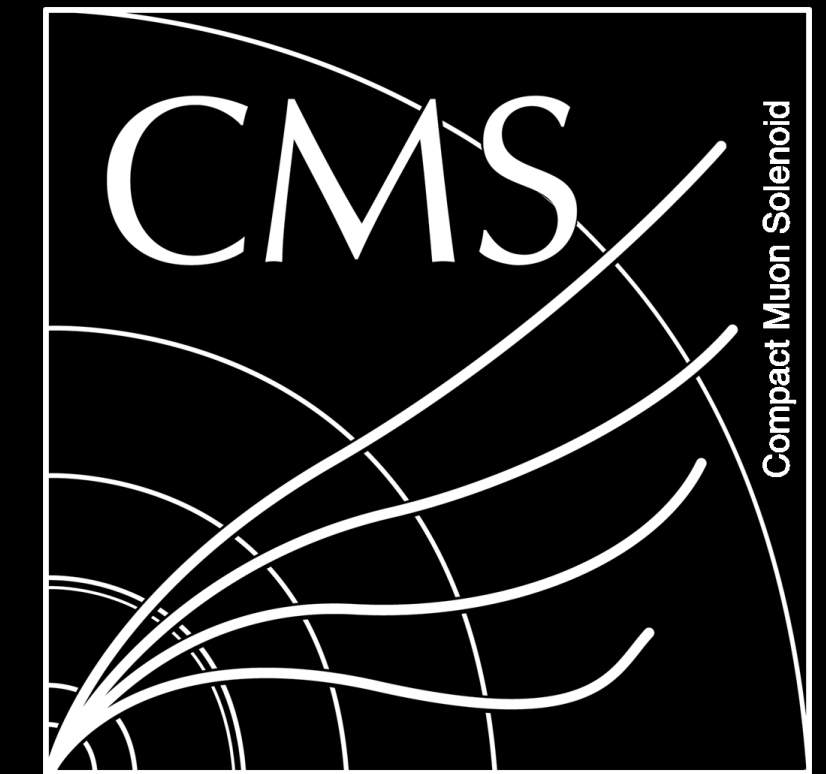


# Search for

$$H \rightarrow \gamma^* \gamma \rightarrow \mu\mu\gamma$$

with full LHC Run-2 data collected by the CMS detector

John Adams Villamoran, Cheng-Han Wu, Hao-Ren Jheng, Chia-Ming Kuo, and Saba Taj  
for the CMS Collaboration



Department of Physics & Center for High-Energy and High-Field Physics, National Central University, Chungli, Taiwan

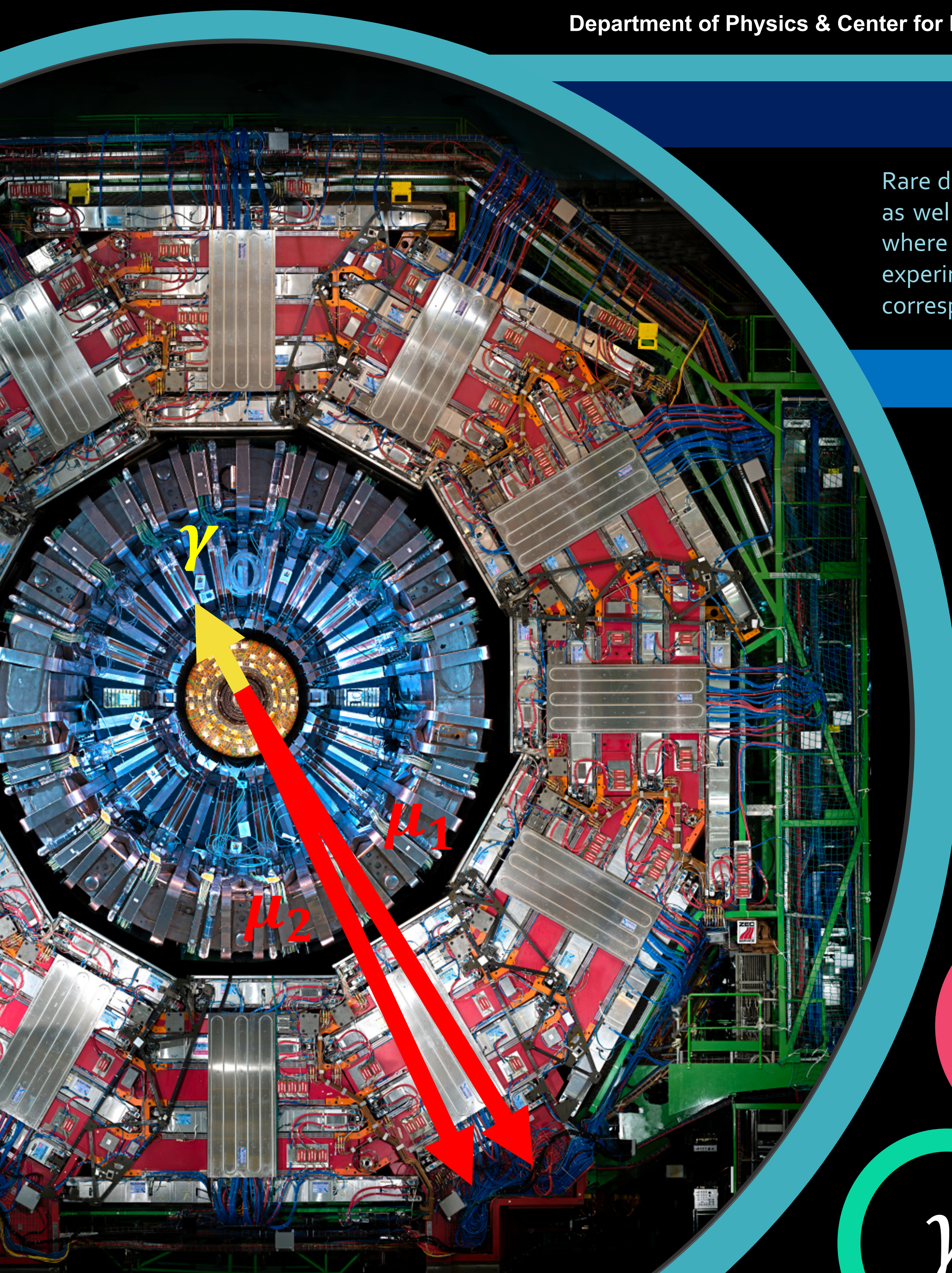


Figure 2. CMS detector cross-sectional view with arrows illustrating the final state signature of  $H \rightarrow \gamma^* \gamma \rightarrow \mu\mu\gamma$ . Image taken from [3]

## Abstract

Rare decays of the Higgs, such as the loop-induced Dalitz process,  $H \rightarrow \gamma^*\gamma$ , provide opportunities to test the Standard Model (SM) as well as multiple theories Beyond the Standard Model (BSM). The topic to be presented discusses the search for the  $H \rightarrow \gamma^*\gamma$ , where an internal conversion of a virtual photon to two muons occurred. Data used in the analysis was collected by the CMS experiment at the LHC from proton-proton collisions with a center-of-mass energy of 13 TeV during the full Run-2 period, corresponding to an integrated luminosity of  $137 \text{ fb}^{-1}$ .

## Introduction

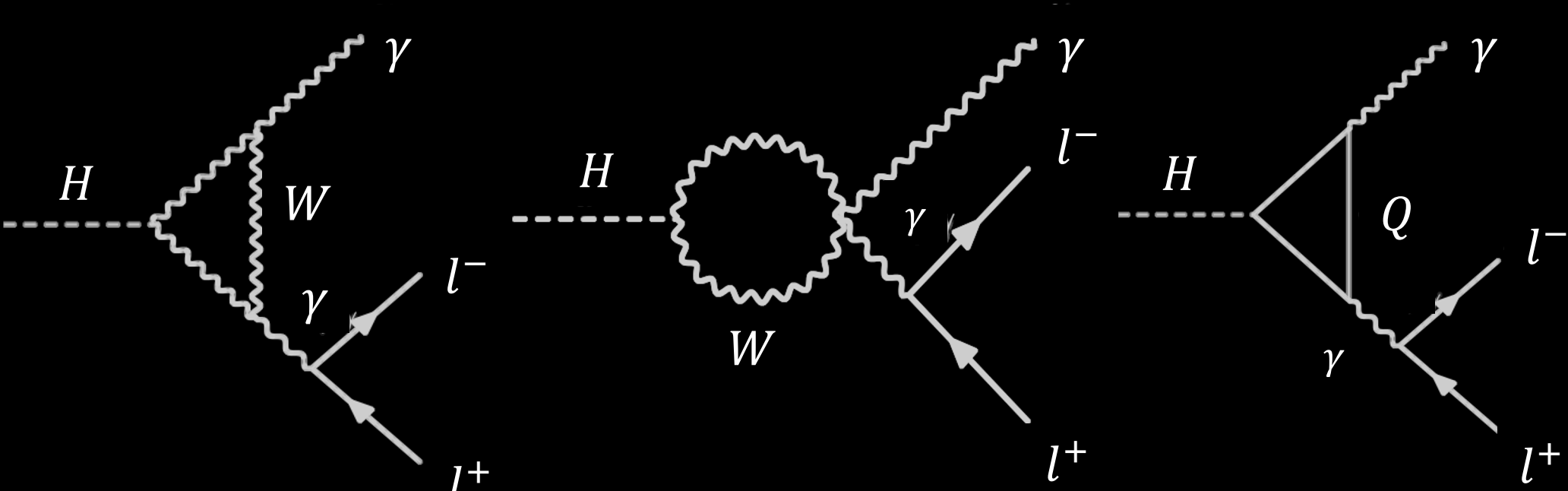
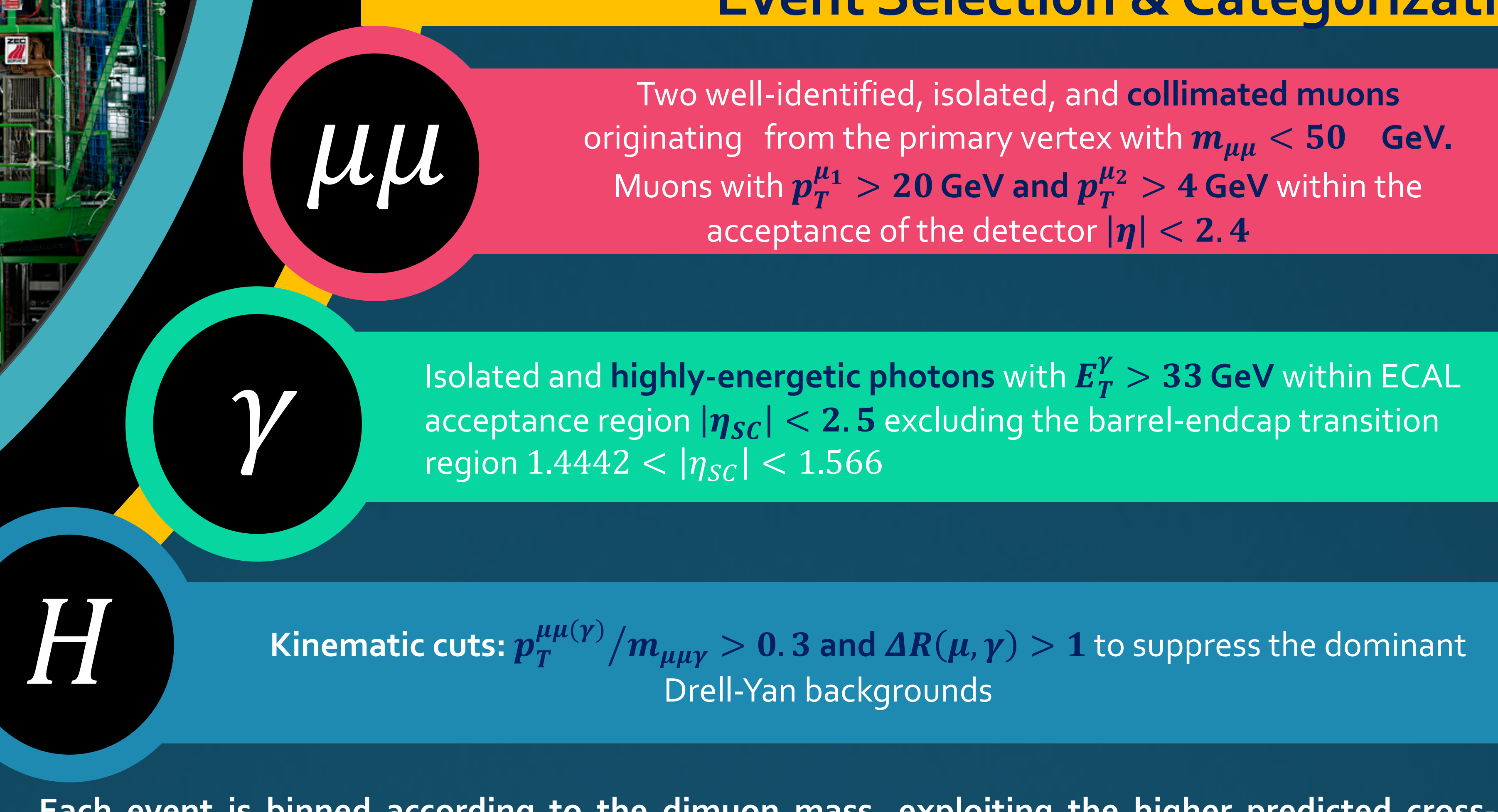


Figure 1. Higgs Dalitz decay loop-induced Feynman diagrams.

Rare Higgs decays in the Standard Model open up a lot of possibilities to investigate physics Beyond the Standard Model (BSM). The Dalitz sector of Higgs decays,  $H \rightarrow ll\gamma$ , are rare decays dominated by loop-induced processes, such as the  $H \rightarrow \gamma^*\gamma$ . This process may possibly be enhanced in some BSM theories, which makes it sensitive to new physics<sup>[1]</sup>. Furthermore, the non-triviality of its angular correlations may result in a nonzero measurement of the forward-backward asymmetry, manifested through CP violation in the  $H_{ll}$  effective coupling<sup>[2]</sup>.

## Event Selection & Categorization



Each event is binned according to the dimuon mass, exploiting the higher predicted cross-section for smaller masses. Each dimuon mass bin is then categorized into the following:

Dijet-tagged 1	Dijet-tagged 2	Boosted-tagged	EB-HR9	EB-LR9	EE
2 jets passing the dijet selection with $m_{jj} > 500 \text{ GeV}$	2 jets passing the dijet selection with $360 < m_{jj} < 500 \text{ GeV}$	Did not pass the dijet-tagged category with $p_T^{\mu\mu\gamma} > 60 \text{ GeV}$	Did not pass the tagged selections with photon in the EB region with $R_9 > 0.96$	Did not pass the tagged selections with photon in the EB region with $R_9 < 0.96$	Did not pass the tagged selections with photon in the EE region

## Signal & Background Modeling

Model the signal using events selected from dedicated signal samples simulating the  $H \rightarrow \gamma^* \gamma \rightarrow \mu\mu\gamma$ . A **maximum-likelihood fit to the three-body invariant mass** was performed using a *Double-Sided Crystal Ball Function*. The resulting fit parameters are then *interpolated* linearly to obtain the signal fits for the intermediate mass points.

The background is modeled using a *data-driven* approach. A **maximum likelihood fit is performed on sideband region of the three-body invariant mass distribution** of the data while blinding the signal region defined in the range  $120 < m_{\mu\mu\gamma} < 130 \text{ GeV}$ . The background fit function is chosen from a list of candidate family functions. An f-test was done to choose a *sufficient order* for each family of functions. An *uncertainty due to the choice of the fit function* is assigned through the envelope method.

Figure 4. (Top) Signal fit for a 125-GeV Higgs boson produced with gluon-gluon fusion in the EB-High R9 category for 2018. (Middle) Signal fit interpolation assuming different Higgs boson masses (120-130 GeV) for 2018 EB-High R9 category. (Bottom) Fit functions chosen by the f-test for 2018 data in the EB-High R9 category.

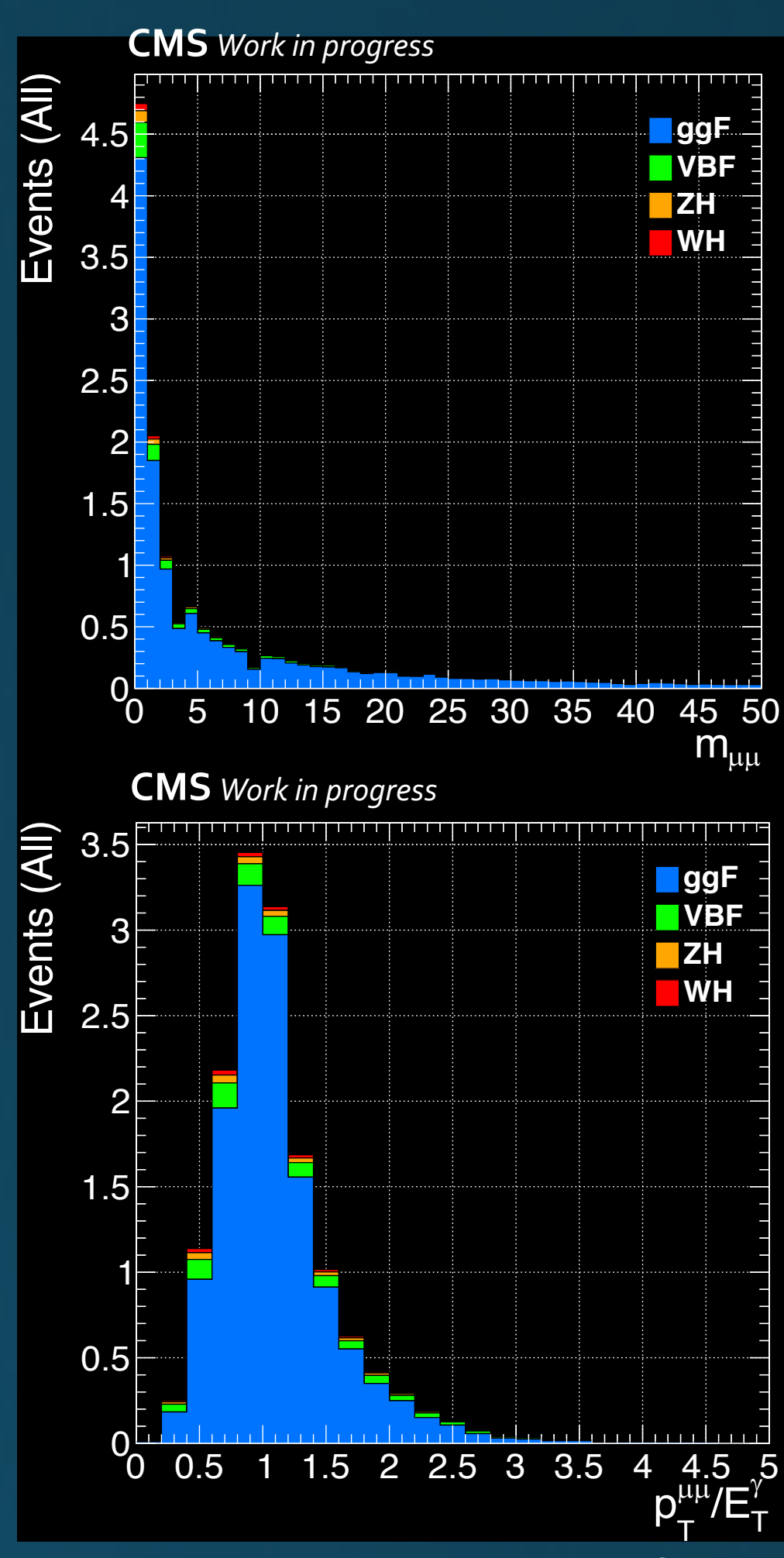


Figure 3. Signal distributions for the dimuon invariant mass (top) and the ratio between the photon and dimuon  $p_T$  (bottom).

## Results & Conclusion

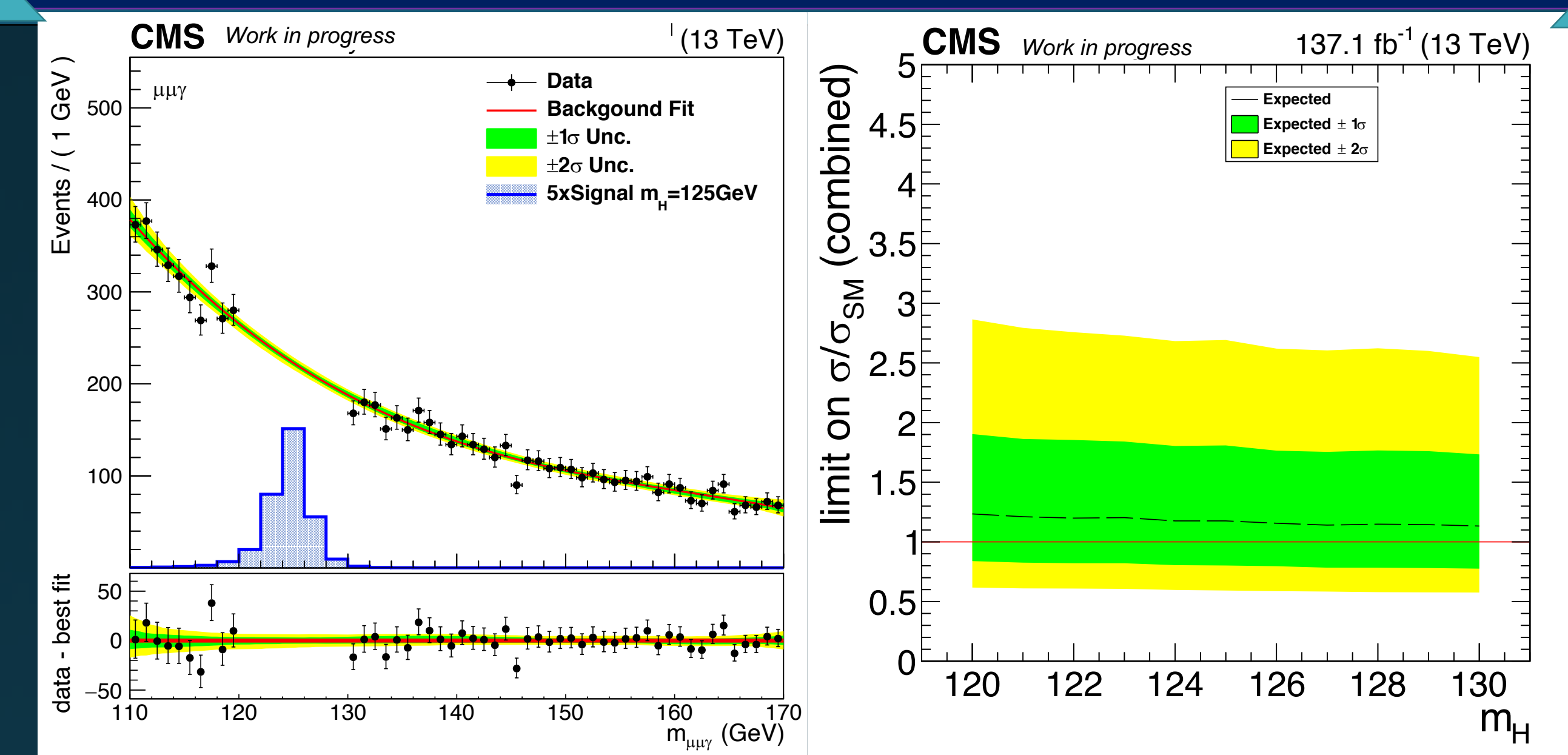


Figure 5. (Left) Final background model with signal histogram (enhanced by a factor of 5 for visualization). (Right) Combined expected upper limits on  $\sigma/\sigma_{SM}$  for all years.

The derived expected upper limit on the ratio of the cross-section times branching with the Standard Model prediction ( $\sigma/\sigma_{SM}$ ) for  $H \rightarrow \gamma^*\gamma \rightarrow \mu\mu\gamma$  at 95% confidence level is  $\sim 1.18$ . This level of sensitivity was achieved by exploiting the special signatures of the decay as well as the multiple categories implemented based on the dimuon invariant mass.

## References

- [1] M. Carena, I. Low, and C. E. M. Wagner, "Implications of a modified higgs to diphoton decay width", *Journal of High Energy Physics* 2012 (Aug, 2012) 60,
- [2] A. Y. Korchin and V. A. Kovalchuk, "Angular distribution and forward-backward asymmetry of the higgs-boson decay to photon and lepton pair", *The European Physical Journal C* 74 (Nov, 2014) 3141
- [3] <https://home.cern/science/experiments>